BIBLIOGRAPHIC INFORMATION SYSTEM

Journal Full Title: Journal of Biomedical Research & Environmental Sciences
Journal NLM Abbreviation: J Biomed Res Environ Sci
Journal Website Link: https://www.jelsciences.com
Journal ISSN: 2766-2276
Category: Multidisciplinary
Subject Areas: Medicine Group, Biology Group, General, Environmental Sciences
Topics Summation: 130
Issue Regularity: Monthly
Review Process: Double Blind
Time to Publication: 21 Days
Indexing catalog: Visit here
Publication fee catalog: Visit here

DOI: 10.37871 (CrossRef)
Plagiarism detection software: iThenticate
Managing entity: USA
Language: English
Research work collecting capability: Worldwide
Organized by: SciRes Literature LLC

IndexCopernicus ICV 2020: 53.77

Manuscript should be submitted in Word Document (.doc or .docx) through

Online Submission

form or can be mailed to support@jelsciences.com

Vision: Journal of Biomedical Research & Environmental Sciences main aim is to enhance the importance of science and technology to the scientific community and also to provide an equal opportunity to seek and share ideas to all our researchers and scientists without any barriers to develop their career and helping in their development of discovering the world.

JOURNAL OF BIOMEDICAL RESEARCH & ENVIRONMENTAL SCIENCES
issn: 2766-2276
SUBJECT AREA(S): ECOTOXICOLOGY | ENVIRONMENTAL CONTAMINATION
DOI: 10.37871

RESEARCH ARTICLE

Photocatalytic Degradation of Polyphenols and Polyaromatic Amines in Textile Industry Wastewaters by Nano-Cerium Dioxide Doped Titanium Dioxide and the Evaluation of Acute Toxicity Assays with Microtox and *Daphnia magna*

Rukiye Öztekin* and Delia Teresa Sponza

Department of Environmental Engineering, Engineering Faculty , Tınaztepe Campus, Dokuz Eylül University, 35160 Buca/Izmir, Turkey

ABSTRACT

In this study, nano-cerium dioxide doped titanium-dioxide (CeO_2-TiO_2) Nanocomposites (NCs) was used for the photocatalytic degradation of pollutant parameters (color, polyphenols, polyaromatics) from a textile industry wastewater (TI ww) treatment plant located in Izmir, Turkey, at different operational conditions such as at increasing photocatalytic time (0, 10, 15, 20, 30, 60, 90 and 120 min), at different CeO_2-TiO_2 mass ratios (1%, 3%, 5%, 10%, 15%, 16%, 25%, 30%, 50%), at the different amounts of CeO_2 (1, 3, 5, 8, 10, 15, 20 and 25 mg/L) under 130 W Ultraviolet (UV) and 35 W sun lights irradiations, respectively. Color, polyphenols (quercetin, fisetin, ellargic acid, carminic acid, luteolin, and curcumin) and polyaromatics [2,6-dimethylaniline (2,6-DMA), 2-aminoanisole (MOA), 2,4-toluenediamine (TDA), 2-naphthylamine (NA), 4,40-thiobisbenzenamine (TOA), 3,3-dichlorobenzidine (DCB) and 3,30-dimethoxybenzidine (DMOB)] removal efficiencies were observed between 78% and 99% during photocatalytic experiments, under 130 W UV light, at 15% CeO_2-TiO_2 NCs, at 21°C, after 30 min irradiation time. 15% CeO_2-TiO_2 NCs shows the highest photodegradation yield of color under both UV and visible-light irradiation, with maximum photo-degradation rates of 99% and 98.5%, respectively, after 30 min irradiation time. 94.44% maximum Microtox acute toxicity yield was found in CeO_2-TiO_2 NCs = 20 mg/L, at 5% CeO_2 mass ratio, after 150 min photodegradation time at 60°C. 90% maximum *Daphnia magna* acute toxicity removal was obtained in CeO_2-TiO_2 NCs = 20 mg/L, at 5% CeO_2 mass ratio, after 150 min photodegradation time at 60°C. The results show that the CeO_2-TiO_2 NCs has a high photocatalytic activity to remove the pollutants from TI ww.

Introducion

In recent years, Advanced Oxidation Processes (AOPs) have emerged as potentially powerful methods that are capable of transforming the pollutants into harmless substances [1] and that almost all rely on the generation of very reactive free radicals, such as the hydroxyl radical ($OH^{\bullet}$) (redox potential = 2.8 V) [2]. AOPs, generally involving H_2O_2, O_3 or Fenton's reagent as oxidative species for the destruction of contaminants, are alternative techniques to eliminate dyes and other organics in wastewater [3-7]. Semiconductor photocatalysis has emerged

***Corresponding author(s)**

Rukiye Öztekin, Department of Environmental Engineering, Engineering Faculty , Tınaztepe Campus, Dokuz Eylül University, 35160 Buca/Izmir, Turkey

Tel: +90-232-301-7119
Fax: +90-232-453-1143
E-mail: rukiyeoztekin@gmail.com

DOI: 10.37871/jbres1524

Submitted: 03 August 2022

Accepted: 08 August 2022

Published: 09 August 2022

Keywords

Cerium dioxide doped titanium dioxide nanocomposites; *Daphnia magna* and Microtox (with *Aliivibrio fischeri or Vibrio fischeri*) acute toxicity tests; Polyaromatics; Polyphenols; Textile industry wastewater

ENVIRONMENTAL SCIENCES
ECOTOXICOLOGY | ENVIRONMENTAL CONTAMINATION
VOLUME: 3 ISSUE: 8 - AUGUST, 2022

How to cite this article: Öztekin R, Sponza DT. Photocatalytic Degradation of Polyphenols and Polyaromatic Amines in Textile Industry Wastewaters by Nano-Cerium Dioxide Doped Titanium Dioxide and the Evaluation of Acute Toxicity Assays with Microtox and *Daphnia magna*. J Biomed Res Environ Sci. 2022 Aug 09; 3(8): 852-866. doi: 10.37871/jbres1524, Article ID: JBRES1524, Available at: https://www.jelsciences.com/articles/jbres1524.pdf

as a promising AOP that provides solutions to many environmental pollution problems [3,5-7].

As an important semiconductor material, TiO_2 has been widely used as the photocatalyst because of its chemical and biological inertness, high stability against photocorrosion, non-toxicity, low cost, and excellent degradation for organic pollutants [8,9]. However, practical applications of the TiO_2 are still quite limited, mainly due to the low quantum efficiency and the broad bandgap responding only to UV light [10]. In order to improve the photocatalytic properties of TiO_2, much effort has been made, including transitional metal ion or non metal element doping [11,12], co-deposition of metals [13] and dye sensitization [14].

Cerium oxide and CeO_2 containing materials have been studied as a good alternative for the oxidation catalysts and supports. It has been shown that, when associated with transition metal oxides and noble metals, cerium oxide promotes oxygen storage and release to enhance oxygen (O_2) mobility, and forms surface and bulk vacancies to improve the catalyst redox properties of the system [15,16].

Among them, coupling TiO_2 with CeO_2 attracts much attention because of the special f and d electron orbital structure and the special properties of CeO_2 [16]. It has been found that the variable valences of Ce such as Ce^{4+} and Ce^{3+} make CeO_2 possesses the excellent characteristics in transferring electrons and enhance the light absorption capability in near UV or UV [17]. Meanwhile, doping with CeO_2 can double oxygen reserve and transfer capacity of the TiO_2 photocatalysis [18]. Introducing CeO_2 into the TiO_2 framework could effectively extend the visible light response of TiO_2 [19]. Many researchers have focused on preparing meso-structured CeO_2-TiO_2 NCs with a large surface area and controllable pore size to improve its photocatalytic activity [19]. The large surface area would improve the absorption and mass-transfer of target pollutants [20].

Pirkami, et al. [21] found 70% Reactive Red 19, 75% Acid Orange 7, and 74% Acid Red 18 removals with 30 mg/L nano-Ni-TiO_2 photocatalyst at pH = 7.0 and 25 C. Shao, et al. [22] studied the photocatalytic degradation of Methylene Blue (MB) dye with the addition of photocatalyst carbon-based anatase-type TiO_2 (TiO_2-C) hybrid aerogel NCs. The photocatalytic degradation removal at darkness condition was found as 33% for MB removal while the MB photodegradation removal was found as 98%, at 500 W UV light, after 150 min at TiO_2/C mass ratio of 0.902, at 25°C [22]. Subramonian and Wu [23] found that 85.2% of 60 mg/L of MB was successfully decolorized under 1.0 g/L of TiO_2 Nanoparticles (NPs) dosage and initial pH 10.5, under sun light irradiation. Ji, et al. [24] reported that CeO_2 NPs powder and light irradiation, 98% of acid orange 7 (AO7) was decolorized at the irradiation time of 11 h. CeO_2 NPs, which were used as a photocatalyst in decolorization of Reactive Orange 16 dye, were synthesized by the microemulsion method and were able to decolorize the aqueous solution after 2 h [25]. At a reaction temperature of 100°C and an initial pH of 5.0, was provided 98.1% color removal, 89.6% COD and 65.4% TOC reduction with 1 mg/L TiO_2–CeO_2 NCs catalyst [26]. The 10% CeO_2-TiO_2 NCs sample shows the highest photoactivity under both UV and visible-light irradiation, with the degradation rate of 95.3% and 57.5%, respectively [27]. Ameen, et al. [28] reported that the CeO_2-TiO_2 NCs as photocatalyst accomplished enormously high degradation of bromophenol (Bph) dye by nearly 72% within 3 h under visible-light (300 W Xe non arc lamp) illumination. Li, et al. [20] synthesized thermally stable mesoporous ZrO_2-CeO_2-TiO_2 NCs and demonstrated the photodegradation of rhodamine B dye by 90% within 160 min under visible light. The photocatalytic studies performed with real TI ww until now were not concern the photo-removals of polyphenols and polyaromatics using CeO_2-TiO_2.

In the present study, CeO_2-TiO_2 NCs was firstly used for the photocatalytic degradation of pollutant parameters (color, polyphenols, polyaromatics) from the TI ww treatment plant in Izmir, Turkey, at different operational conditions such as at increasing photocatalytic time (0, 10, 15, 20, 30, 60, 90 and 120 min), at different CeO_2-TiO_2 mass ratios (1%, 3%, 5%, 10%, 15%, 16%, 25%, 30%, 50%), at the different amounts of CeO_2 (1, 3, 5, 8, 10, 15, 20 and 25 mg/L) under 130 W UV light and 35 W sun light irradiations and at 21°C, respectively. Color, polyphenols (quercetin, fisetin, ellargic acid, carminic acid, luteolin, and curcumin) and polyaromatics [2,6-dimethylaniline (2,6-DMA), 2-aminoanisole (MOA), 2,4-toluenediamine (TDA), 2-naphthylamine (NA), 4,40-thiobisbenzenamine (TOA), 3,3-dichlorobenzidine (DCB) and 3,30-dimethoxybenzidine (DMOB)] removal efficiencies were observed during photocatalytic experiments. Therefore, the acute toxicity assays of TI ww samples with the addition of CeO_2-TiO_2 NCs was evaluated with Microtox (*Vibrio fischeri*) and *Daphnia magna* acute toxicity tests.

Materials and Methods

Raw wastewater

The TI ww used in this study contains color (> 70 1/m), total phenol (> 233 mg/L), COD_{dis} (> 770 mg/L) and high BOD_5 (> 251 mg/L) concentrations with a BOD_5/COD_{dis} ratio of 0.39. The characterization of TI ww was shown in table 1 for minimum, medium and maximum values.

Operational conditions

The operational conditions were summarized in table 2. Time (0, 10, 15, 20, 30, 60, 90 and 120 min), at different CeO_2-TiO_2 mass ratios (1%, 3%, 5%, 10%, 15%, 16%, 25%, 30%, 50%), at the different amounts of CeO_2 (1, 3, 5, 8, 10, 15, 20 and 25 mg/L) under 130 W UV and 35 W sun lights irradiations, respectively. Color, polyphenols (quercetin, fisetin, ellargic acid, carminic acid, luteolin, and curcumin) and polyaromatics [2,6-dimethylaniline (2,6-

Table 1: Characterization values of TI ww (n = 3, mean values ± SD).

Parameters	Values		
	Minimum	Medium	Maximum
pH	5.10 ± 0.18	5.65 ± 0.20	6.20 ± 0.22
DO (mg/L)	1.32 ± 0.05	1.43 ± 0.05	1.54 ± 0.05
ORP (mV)	86.00 ± 3.01	107.55 ± 3.76	129.10 ± 4.52
TSS (mg/L)	286.00 ± 10.01	360 ± 12.6	434.00 ± 15.20
TVSS (mg/L)	193.00 ± 6.8	242.10 ± 8.47	291.20 ± 10.2
COD_{total} (mg/L)	932.60 ± 32.62	1171.40 ± 41.00	1410.10 ± 49.40
$COD_{dissolved}$ (mg/L)	771.30 ± 27.00	968.8 ± 33.91	1166.30 ± 40.82
TOC (mg/L)	463.30 ± 16.22	582.90 ± 20.40	702.40 ± 24.60
BOD_5 (mg/L)	252.60 ± 8.84	315.4 ± 11.04	378.20 ± 13.24
BOD_5/COD_{dis}	0.37 ± 0.02	0.39 ± 0.014	0.41 ± 0.02
Total N (mg/L)	25.70 ± 0.90	30.96 ± 1.08	36.22 ± 1.27
NH_4-N (mg/L)	1.87 ± 0.07	2.25 ± 0.08	2.63 ± 0.092
NO_3-N (mg/L)	8.10 ± 0.28	10.2 ± 0.36	12.20 ± 0.43
NO_2-N (mg/L)	0.14 ± 0.005	0.16 ± 0.006	0.18 ± 0.006
Total P (mg/L)	8.90 ± 0.31	11.05 ± 0.39	13.20 ± 0.46
PO_4-P (mg/L)	6.34 ± 0.22	8.03 ± 0.28	9.72 ± 0.34
SO_4^{-2} (mg/L)	1250.10 ± 43.80	1560.8 ± 54.63	1871.40 ± 65.50
Color (1/m)	71.80 ± 2.51	89.05 ± 3.12	106.30 ± 3.72
Total phenol (mg/L)	234.00 ± 8.19	702.00 ± 24.57	936.00 ± 32.76
TAAs (mg benzidine / L)	1790.20 ± 62.66	3580.14 ± 125.31	5370.10 ± 188.00

Table 2: Operational conditions under 130 W UV and 35 W sun light irradiations.

Parameters				
Time (min)	CeO_2-TiO_2 NCs mass ratios (%)	CeO_2 NPs (mg/L)	Polyphenols	Polyaromatics
0	1%	1	quercetin	2,6-dimethylaniline (2,6-DMA)
10	3%	3	fisetin	2-aminoanisole (MOA)
15	5%	5	ellargic acid	2,4-toluenediamine (TDA)
20	10%	8	carminic acid	2-naphthylamine (NA)
30	15%	10	luteolin	4,40-thiobisbenzenamine (TOA)
60	16%	15	curcumin	3,3-dichlorobenzidine (DCB)
90	25%	20		3,30-dimethoxybenzidine (DMOB)
120	30%	25		
	50%			

DMA), 2-aminoanisole (MOA), 2,4-toluenediamine (TDA), 2-naphthylamine (NA), 4,40-thiobisbenzenamine (TOA), 3,3-dichlorobenzidine (DCB) and 3,30-dimethoxybenzidine (DMOB)] removal efficiencies were observed during photocatalytic experiments.

Analytical methods

pH, T(˚C), ORP (mV), TSS, TVSS, DO, BOD_5, COD_{total}, $COD_{dissolved}$ and TOC were monitored following Standard Methods 2550, 2580, 2540 C, 2540 E, 5210 B, 5220 D, 5310, 5520 B, respectively [29]. Total-N, NH_4-N, NO_3-N, NO_2-N, Total-P, PO_4-P, total phenol and SO_4^{-2} were measured with cell test spectroquant kits (Merck, Germany) at a spectroquant NOVA 60 (Merck, Germany) spectrophotometer (2003). The characterization of TI ww was shown in table 1 for minimum, medium and maximum values.

Gas Chromatography/Mass Spectrometry (GC/MS) was used for the identification, Gas Chromatography Nitrogen Phosphorous Detection (GC-NPD) for the quantification and Gas Chromatography Flame İonization Detection (GC-FID) for the determination of purity. The base peak of DCB, N-acetyl-DCB and N,N'-diacetyl-DCB was 252 m/z. The other main peaks were 294 m/z for N-acetyl-DCB, and 294 and 336 m/z for N,N'-diacetyl-DCB.

Polyphenols measurement was performed following the Standard Methods 5520 B [29] with a Gas Chromatography-Mass Spectrometry (GC-MS) (Hewlett-Packard 6980/HP5973MSD). Mass spectra were recorded using aVGTS 250 spectrometer equipped with a capillary SE 52 column (0.25 mm ID, 25 m) at 220˚C with an isothermal program for 10 min. The total phenol was monitored as follows: 40 mL of TI ww was acidified to pH = 2.0 by the addition of concentrated HCl. Phenols were then extracted with ethyl acetate. The organic phase was concentrated at 40˚C to about 1 mL and silylized by the addition of N,O-bis (trimethylsilyl) acetamide (BSA). The resulting trimethylsilyl derivatives were analysed by GC-MS (Hewlett-Packard 6980/HP5973MSD). Polyphenols such as quercetin, fisetin, ellargic acid, carminic acid, luteolin, curcumin and polyaromatics such as 2,6-DMA, MOA, TDA, NA, TOA, DCB and DMOB were determined GC-MS (Hewlett-Packard 6980/HP5973MSD).

Preparation of nano CeO_2 - TiO_2 NCs under laboratory conditions

0.3 g of cerium nitrate ($Ce(NO_3)_3.6H_2O$, 98.5%, Daejung chemicals) was dispersed in 20 mL ethanol (C_2H_5OH) and a separate solution of titanium butoxide (97%, Sigma-Aldrich) in a mixture of ethanol:deionized water (DI H_2O) (20 mL/10 mL) was prepared. Afterwards, both the solutions were mixed and at pH = 10.0 was maintained by the dropwise addition of ammonia solution (NH_3, 98%, Daejung chemicals). The entire reaction solution was transferred into the teflon-beaker and sealed into a stainless steel autoclave and kept at 120˚C for 48 h. After completion of the reaction, the autoclave was cooled at room temperature and the product was filtered, washed thoroughly with DI H_2O, and dried overnight at 80˚C. The as-synthesized material was calcined at 450˚C with the ramp rate of 5˚C/min.

Characterizations

The morphological observations were observed by field emission scanning electron microscope (FESEM, Hitachi S-4700) and transmission electron microscopy (TEM, JEM-2010-JEOL).

All experiments were carried out three times and the results given as the means of triplicate samplings. Individual TI ww concentrations are given as the mean with Standard Deviation (SD) values.

Results and Discussion

Transmission Electron Microscopy (TEM) analysis results

TEM was used to investigate the morphological characterizations of the synthesized CeO_2-TiO_2 NCs. Figure 1a shows bare TiO_2 NPs of spherical morphology with the average particle size of 20 nm. CeO_2-TiO_2 NCs (Figure 1b) displays two distinctive morphologies of large CeO_2 NPs and small TiO_2 NPs. The large CeO_2 NPs are uniformly embedded into TiO_2 NPs, indicating well mixing of CeO_2 into TiO_2 NPs. The embedded large hexagonal CeO_2 NPs along with small TiO_2 NPs are synthesized CeO_2-TiO_2 NCs. The diffraction peaks at 28.3˚, 32.8˚, 47.2˚, 56.1˚ and 69.3˚ are assigned to the cubic fluorite structure of CeO_2 [30]. The diffraction peaks at 25.3˚ corresponds to TiO_2 phase in CeO_2-TiO_2 NCs. The synthesized CeO_2-TiO_2 NCs presents red shift to higher wavelength at 465 nm, indicating the incorporation of Ce cations into the lattice of TiO_2. Further, the band gap (Eg) value of 2.67 eV for CeO_2-TiO_2 NCs is lower than bare TiO_2 (Eg = 3.18 eV) which again confirms the incorporation of CeO_2 into TiO_2 NPs (data not shown). The lowering in Eg value of CeO_2-TiO_2 NCs is an indication of the red shifting from UV to the visible region due to the substitution of Ti^{4+} cations by Ce^{4+} cations in TiO_2 network as well as by Ti^{4+} titanium deficiency created per unit cell [V^{1+} Ti^{4+}] as reported by [30].

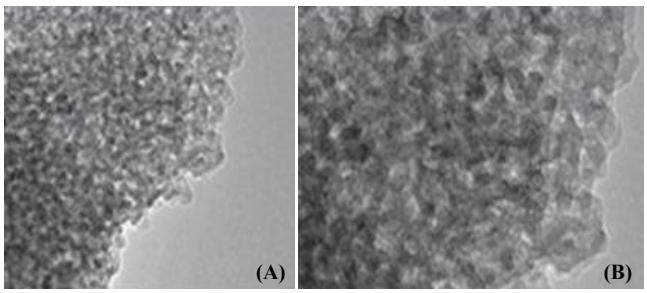

Figure 1 a). Bare TiO_2 NPs of spherical morphology with the average particle size of 20 n.
b). Two distinctive morphologies of large CeO_2 NPs and small TiO2 NPs.

X-rays Diffraction (XRD) analysis results

Figure 2a shows (XRD) of synthesized CeO_2-TiO_2 NCs. The diffraction peaks at 28.3˚, 32.8˚,47.2˚, 56.1˚ and 69.3˚ are assigned to the cubic fluorite structure of CeO_2 [30]. The diffraction peaks at 25.3˚ corresponds to TiO_2 phase in CeO_2-TiO_2 NCs. Figure 2b shows the ultraviolet-diffused reflectance spectroscopy (UV-DRS) of bare TiO_2 and CeO_2-TiO_2 NCs. The characteristic absorption band at 390 nm corresponds to $O_2^{1-\bullet}$, Ti^{4+} charge transfer and related to electron excitation from valence band to the conduction band in TiO_2 [30]. The synthesized CeO_2-TiO_2 NCs presents red shift to higher waveleng that 465 nm, indicating the incorporation of Ce cations into the lattice of TiO_2. Further, the band gap (Eg) value of 2.67 eV for CeO_2-TiO_2 NCs is lower than bare TiO_2 (Eg = 3.18 eV) which again confirms the incorporation of CeO_2 into TiO_2 NPs. The lowering in Eg value of CeO_2-TiO_2 NCs is an indication of the red shifting from UV to the visible region due to the substitution of Ti^{4+} cations by Ce^{4+} cations in TiO_2 photooxidation as well as by Ti^{4+} titanium deficiency created per unit cell [V^{1+} Ti^{4+}].

Effect of the amount of CeO_2 loading in the CeO_2-TiO_2 NCs

The photocatalytic activity of TiO_2 NPs was enhanced by

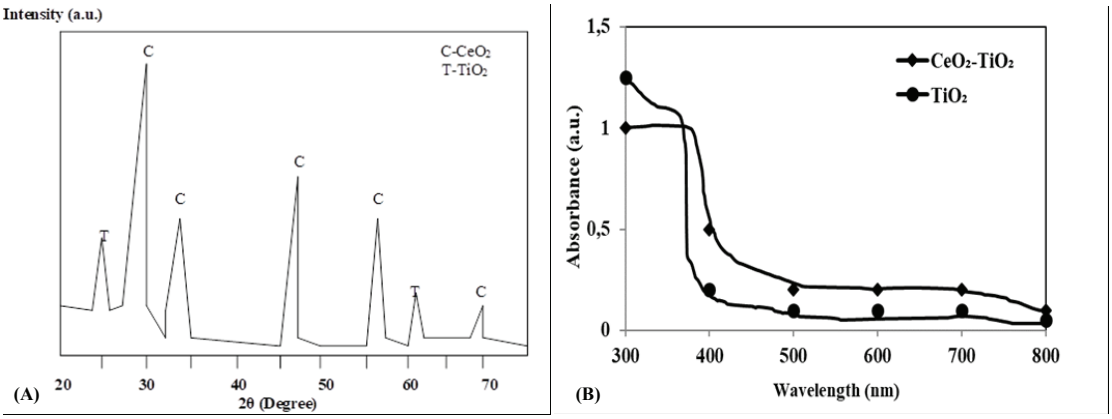

Figure 2 XRD patterns a) and UV-vis spectra b) of CeO_2-TiO_2 NCs.

the addition of CeO_2 from 1 mg/L to 3 mg/L, 5 mg/L, 8 mg/L, 10 mg/L, 15 mg/L, 20 mg/L and 25 mg/L CeO_2 has multi functional role (data not shown). It traps electrons, which retarded electron-hole recombination and increasing $O_2^{1-\bullet}$ for degradation of the pollutants by the Equation 1, Equation 2, Equation 3, Equation 4 and Equation 5:

$$TiO_2 + h_v \rightarrow CB + h + VB \quad (1)$$

$$Ce^{4+} + e^- + CB \rightarrow Ce^{3+} \quad (2)$$

$$Ce^{3+} + O_2^{\bullet} \rightarrow Ce^{4+} + O^{2-\bullet} \quad (3)$$

$$O^{2-\bullet} + 4H^+ \rightarrow 2OH^{\bullet} \quad (4)$$

$$pollutant + OH^{\bullet} \rightarrow degradation\ products \quad (5)$$

The results indicated that the photocatalytic activities increases with increasing the amount of cerium (Ce) dopant until a maximum is reached at 15 wt% (data not shown). This behavior might be associated with the separation of photoinduced electron–hole pairs. Further increasing in Ce content up to 20 wt% leads to a decline in the catalytic activity (data not shown). As the concentration of CeO_2 phase increases, the impurity band would become broader and thus the charge separation gap became narrower and the recombination of electron–hole pairs would be rapid. There are two factors which limited the amount of Ce loading: (i) blockage of active sites by excess amounts of Ce introduced in the photocatalysts and (ii) an increase in opacity and light scattering of CeO_2-TiO_2 NPs at a high concentration leads to a decrease in the passage of irradiation through the sample [31,32].

Efffect of two CeO_2-TiO_2 NCs concentrations with 5% and 15% CeO_2 mass ratios and pure NPs on the photodegradation yields of color under 130 W UV power

The photocatalytic degradation rate of color with 20 mg/L pure CeO_2 NPs, 20 mg/L pure TiO_2 NPs and CeO_2-TiO_2 NCs = 15 mg/L with 5% and 15% CeO_2 mass ratios and CeO_2-TiO_2 NCs = 20 mg/L with 5% and 15% CeO_2 mass ratios, respectively, under 30 min with 130 W UV irradiation are shown in figure 3. This figure demonstrates that the pure TiO_2, pure CeO_2 exhibited low color photodegradation rates (64% and 60%, respectively) since the catalyst could not be effectively activated by visible lights due to big energy band gaps (3.18 eV for TiO_2 and 2.88 eV for CeO_2) (data not shown). Modification of TiO_2 with CeO_2 resulted in abrupt increase of the color photodegradation efficiency owing to the CeO_2-photosensitization as reported by Liu, et al. [27]. However, the yields of color photodegradation increases as well as the concentration of CeO_2 increases from 5% to 15%. The TI ww sample containing 15 mg/L CeO_2-TiO_2 NCs with 15% CeO_2 mass ratio shows the highest photoactivity for color degradation under UV irradiation, with the mineralization rate of 99.3%. 20 mg/L CeO_2-TiO_2 NCs with a CeO_2 mass ratio of 15% exhibited a color photodegradation rate of 82%.

Effect of irradiation times and CeO_2 NPs mass ratios in the CeO_2-TiO_2 NCs on the photooxidation of color in TI ww under UV and sun light irradiations

The maximum color removal yields were observed after 30 min UV and sun light irradiations times with powers of 130 W and 35 W (Figure 3). From figure 4 it can be seen that the photocatalytic activity of prepared CeO_2-TiO_2 NCs increases with the increase of Ce content from 1% to 2%, to 5% and to 15% after 30 min irradiation time at an UV power of 130 W at constant CeO_2-TiO_2 NCs concentrations of 15 mg/L for color photodegradation.

However, the color removals decrease as well as the concentration of CeO_2 NPs increases from 16 to 50%. 15% CeO_2-TiO_2 NCs shows the highest photodegradation yield of color under both UV and visible-light irradiation, with maximum photodegradation rates of 99% and 98.5%, respectively, after 30 min irradiation time (Figures 4,5). This fact is consistent with its smaller particle size, larger surface area, lower concentration of Ce^{3+} and highest concentration of surface Hydroxyl (OH) groups. This can also be attributed

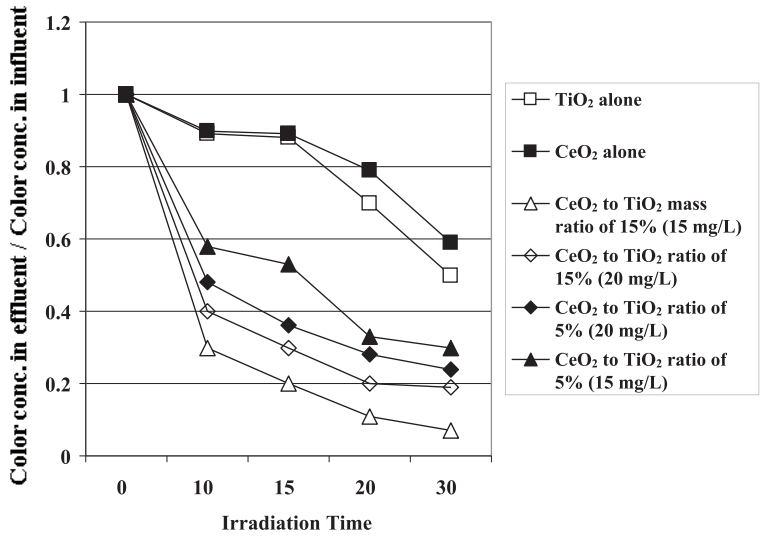

Figure 3 Effects of CeO_2-TiO_2 NCs concentrations and mass ratios of CeO_2 on the TiO_2 to photocatalytic rates of color in the TI ww under 130W UV irradation at original TI ww at pH = 6.2 and at 21°C, respectively.

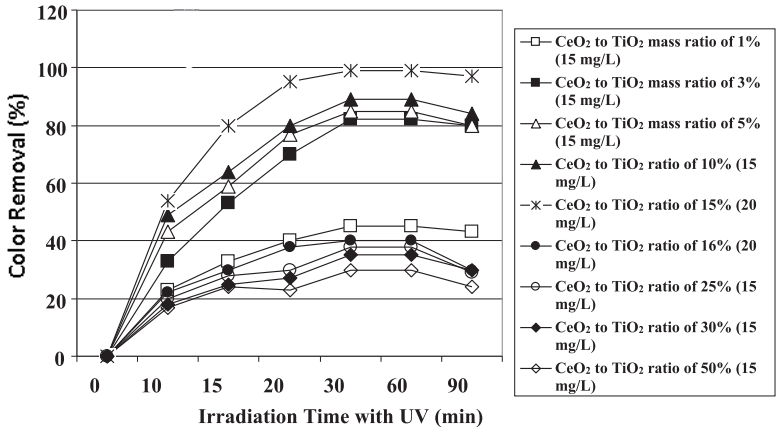

Figure 4 Effect of irradiation time and CeO_2 mass ratios in the CeO_2-TiO_2 NCs on color removal under 130W UV irradiation at original TI ww at pH = 6.2 and at 21°C, respectively.

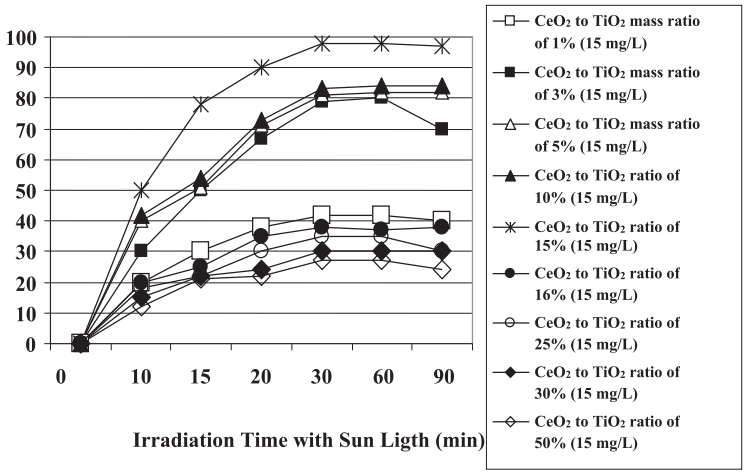

Figure 5 Effect of irradiation time and CeO_2 mass ratios in the CeO_2-TiO_2 NCs on color removal under 35W sun ligth irradiation at original TI ww at pH = 6.2 and at 21°C, respectively.

to the fact that when doping content of CeO_2 NPs is an optimum amount, the CeO_2 NPs well dispersed on the TiO_2 surface can act as electron-hole separation centers. The minimum color removal yields with photodegradation were found for 15 mg/L CeO_2-TiO_2 NCs concentrations with 30% and 50% CeO_2 mass ratios. When the doping CeO_2 NPs concentration exceeds a certain amount (≥ 15%), the trap center may become the recombination center of photo-generated electrons and holes. Meanwhile, the excessive ceria result in agglomeration of CeO_2 NPs, which will scatter the incident light, lowering the photoquantum efficiency of the photocatalytic reaction as reported by Liu, et al. [27]. After 30 min irradiation time the color yield remained constant or decreased sligtly at all CeO_2 to TiO_2 mass ratios.

The majority of color has been degraded within first 28 min. Thus, the synthesized CeO_2-TiO_2 NCs could be a good visible-light driven photocatalyst for the degradation of color originating from the dyes in the TI ww as catalyst under light illumination. The mechanism of color photodegradation can be summarized as follows: Upon 130 W light illumination, CeO_2 firstly absorbs light and the photoexcited electron moves to the Conduction Band (CB) of CeO_2 where CB level is higher than the CB level of TiO_2 NPs. The photoexcited electrons inject into CB of TiO_2 which easily scavenges the electrons to produce the large amount of reactive holes. The existence of mixture of Ce^{3+}/Ce^{4+} oxidation states on the surface of nano CeO_2-TiO_2, denote the NCs is not fully oxidized, so that Ce^{4+} can easily capture electrons and prevent the combination of photo-generated electrons and holes, resulting in a higher quantum efficiency of photocatalytic reaction [33]. Secondly, the photo-induced electrons in the TiO_2 can drift to the CeO_2 under the inner electric field between CeO_2 and TiO_2 due to the energy band bending in space charge region. It is more helpful for the separation of photoinduced electron–hole pairs in TiO_2, resulting in the improvement of photocatalysis under UV illumination [30]. In addition, with the doping of CeO_2, the abundant surface OH groups exist on the surface of TiO_2, which can be attacked by photoinduced holes and yield surface $OH^{\bullet}$ with high oxidation capability [27].

Polyphenols in TI ww

The dyes in the textile industry is the main source of the color. The dyes used to color textiles are flavonoid compounds carotenoids, hydroxyketones, anthraquinones, naphthoquinones, flavones, flavonols, flavonones, indigoids and related compounds. Polyphenolic compounds that are expected to be found in the textile dyes are ellagic acid (simple phenolic acid); catechin, rutin, myricetin, luteolin, kaempferol, apigenin, morin, fisetin (flavonoids); curcumin (curcuminoid), carminic acid, purpurin and alizarin (having a core anthraquione structure). Among these polyphenols; quercetin, fisetin, ellagic acid, carminic acid, luteolin and curcumin concentrations were monitored as color polyphenols in TI ww.

At initial, color exhibits the maximum absorption wavelength at λ = 620 nm after 20 min photodegradation at 130 W UV using CeO_2-TiO_2 NCs = 15 mg/L with 15% CeO_2 mass ratio (Figure 6). The maximum absorption wavelength was 560 nm with only 15 mg/L CeO_2 concentration while the maximum absorption wavelengths were 560 and 580 nm at 15 mg/L pure nano-TiO_2 and pure nano-CeO_2. The absorbance intensity of color gradually decreases with the increase of exposed time from 20 to 30 min, indicating the drastic decrease in the concentration of color originating from dyes in TI ww. The absorption wavelength λ decreased to 110 nm after 30 min for CeO_2-TiO_2 NCs = 15 mg/L with 15% CeO_2 mass ratio while the adsorption wavelenthgs decreased to around 300 nm in both commercial nanoparticles (Figure 6). A reasonably high degradation rate of 99.3% of color within 30 min is detected over the surface of CeO_2-TiO_2 NCs catalyst whereas, very low degradation rates (6% and 23%) is obtained when TI ww degradation takes place over

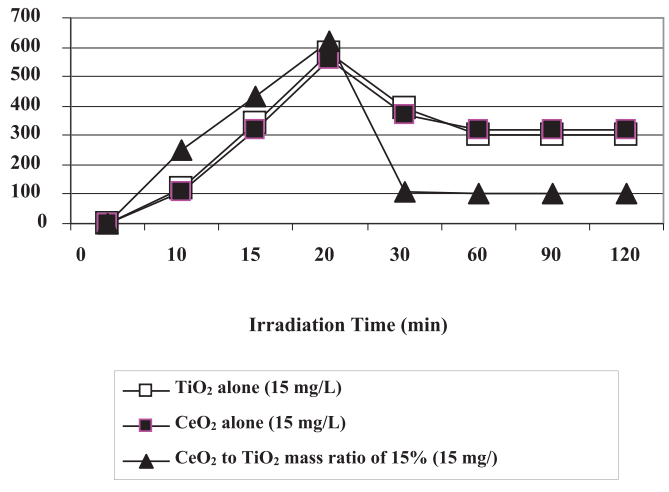

Figure 6 Absorbances of color versus produced NCs and commercial NPs under 130W UV irradiation.

the surface of commercial CeO_2 and TiO_2 catalysts under 130 W UV light illumination. The high color removal efficiency observed in this photocatalytic process is due to the fact that azo bond cleavage is easier in color giving polyphenols.

The maximum polyphenol yields were obtained after 30 min irradiation time under UV (Figure 7). The maximum photooxidation yields for quercetin, fisetin and ellagic acid polyphenols were high (99%; 98% and 97%, respectively) while the yields for carminic acid, luteolin and curcumin polyphenols were sligthly low (88%, 82% and 80%, respectively). The electron orbital structure and the special properties of CeO_2 NPs has been found that the variable valences of Ce such as Ce^{4+} and Ce^{3+} make CeO_2 NPs possesses the excellent characteristics in transfer- ring electrons and enhance the light absorption capability in near ultraviolet or ultraviolet [20]. Meanwhile, doping with CeO_2 NPs can double O_2 reserve and transfer capacity of the TiO_2 NPs photocatalysis [20]. Based on the catalytic mechanism, the increasing O_2 adsorbed on the surface of particle can easily capture electron, which prohibits the undesirable recombination of electron-hole pair and greatly improves the catalytic oxidation activity.

Polyphenol metabolites

From 120 mg/L quercetin; 20 mg/L isorhamnetin (3′-O-methyl quercetin), and 46 mg/L tamarixetin (4′-O-methyl quercetin) produced as metabolites of quercetin polyphenol after 10 min photooxidation with CeO_2-TiO_2 NCs = 15 mg/L at 15% CeO_2 mass ratio (Table 3). From 60 mg/L fisetin polyphenol, 40 mg/L 3',4'-catechol generated. From 80 mg/L ellagic acid, 43 mg/L 3,8-dihydroxy-6H-dibenzopyran-6-one), 15 mg/L 3-Hydroxyurolithin and 10 mg/L 7-Hydroxy-3,4-benzocoumarin produced (Table 3).

The polyphenols transformed by photodegradation of polyphenols by ring cleavage, decarboxylation and dehydroxylation reactions under UV. Carminic acid metabolites were C-glucopyranosyl flavokermesic acid and glucopyranosyl-dioxoanthracene *via* hydroxylation under UV (Table 3). From 120 mg/L carminic acid 30 mg/L C-glucopyranosyl flavokermesic acid and 20 mg/L glucopyranosyl-dioxoanthracene produced. Two methylated isomers of luteolin was observed as luteolin metabolites. Methylation probably occurred on ring to give 3'- or 4'-O-methylluteolin. 3'-methylluteolin and the 4'-methylisomer were found as metabolites of luteolin after 10 min illumination with 130 W UV, at CeO_2-TiO_2 NCs = 15 mg/L at 15% CeO_2 mass ratio. From 80 mg/L luteolin 20 mg/L 3'-methylluteolin and 18 mg/L 4'-methylisomer produced. From 89 mg/L curcumin 34 mg/L bisdemethoxycurcumin (BDMC), 20 mg/L O-glucuronide (COG) and 8 mg/L curcumin O-sulfate (COS) produced after 10 min irradiation.

Quercetin metabolites such as isorhamnetin and tamarixetin removal efficiencies were 98% and 96%, after 30 min irradiation time (Table 3). Fisetin metabolites such as 3'-4'-catechol removal efficiency was 94%, after 30 min irradiation time (Table 3). Ellargic acid metabolites such as 3,8-dihydroxy-6H dibenzopyran-6-one, 3-hydroxyurolithin, 7-hydroxy-3,4-benzocoumarin removal efficiencies were 90%, 93%, and 94%, respectively, after 30 min irradiation time (Table 3). Carminic acid metabolites such as C-glucopyranosyl flauokermesic, glucopyranosyl-dioxoanthracene removal efficincies were 84% and 86%, after 30 min irradiation time (Table 3). Luteolin metabolites such as 3'-methylluteolin, 4'-methylisomer removal efficiencies were 80% and 78%, after 30 min irradiation time (Table 3). Curcumin metabolites such as bisdemethoxycurcumin, o-glucuronide, curcumin o-sulfate removal efficiencies were 78%, 74%, and 72%, respectively, after 30 min irradiation time (Table 3).

Aromatic amines in TI ww

Figure 8 shows the UV-Vis absorbance of individual aromatic amines with the exposed time of 0-120 min. After

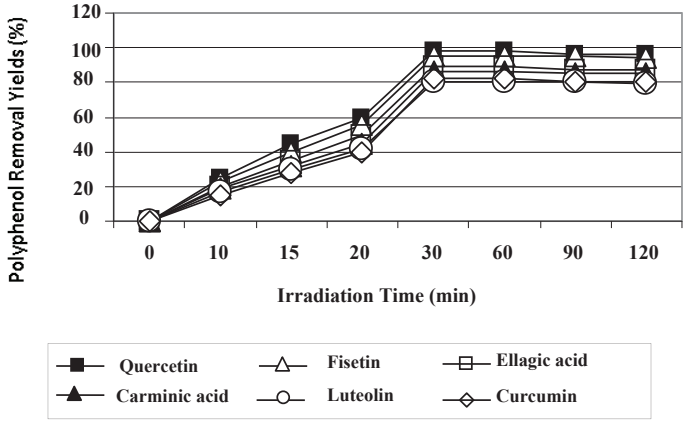

Figure 7 Removals of polyphenols via photooxidation using CeO_2-TiO_2 NCs = 15 mg/L with 15% CeO_2 mass ratio, under 130W UV, at pH = 6.2 and at 21°C, respectively.

Table 3: Removal efficiencies of polyphenol metabolites after 10 min and 30 min irradiation with CeO_2-TiO_2 NCs under 130 W UV power.

Polyphenol Metabolites		After 10 min		After 30 min		
Names	Influent Conc. (mg/L)	Ce_2O_2-TiO_2 NCs Conc. (mg/L)	Rem. Yields (%)	Ce_2O_2-TiO_2 NCs Conc. (mg/L)	Rem. Yields (%)	Remaining conc. (mg/L)
Quercetin metabolites						
Isorhamnetin	20	15.6	22	0.4	98	0.4
Tamarixetin	46	36.34	21	1.84	96	1.84
Fisetin metabolites						
3'-4'-catechol	40	30	25	2.4	94	2.4
Ellagic acid metabolites						
3, 8-dihydroxy-6H dibenzopyran-6-one	43	32.25	25	4.3	90	4.3
3-hydroxyurolithin	15	12	20	1.05	93	1.05
7-hydroxy-3,4-benzocoumarin	10	7.8	22	0.6	94	0.6
Carminic acid metabolites						
C-glucopyranosyl flauokermesic	30	24.3	19	4.8	84	4.8
Glucopyranosyl-dioxoanthracene	20	15.2	24	2.8	86	2.8
Luteolin metabolites						
3'-methylluteolin	20	16.2	19	4	80	4
4'-methylisomer	18	14.22	21	3.96	78	3.96
Curcumin metabolites						
Bisdemethoxycurcumin	34	27.88	18	7.48	78	7.48
O-glucuronide	20	16	20	5.2	74	5.2
Curcumin O-sulfate	8	6.16	23	2.24	72	2.24

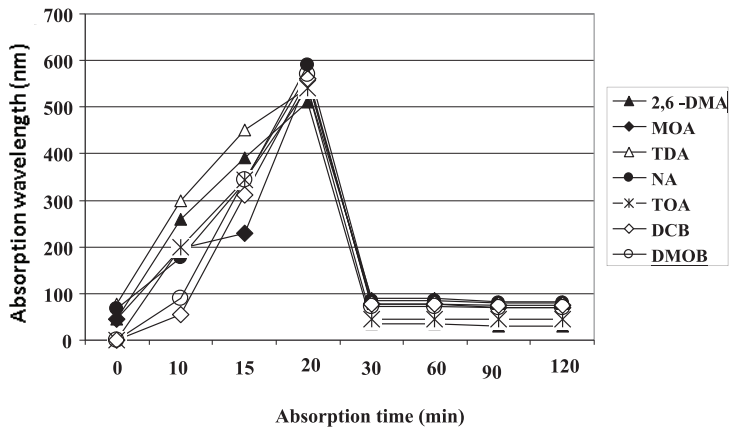

Figure 8 UV-vis absorbances of individual aromatic amines after photodegradation at 130W UV power using 15 mg/L CeO_2-TiO_2 NCs with 15% CeO_2 mass ratio, at pH = 6.2 and at 21°C.

20 min photooxidation the aromatic amines namely 2,6-DMA, MOA, TDA, NA, TOA, DCB and DMOB exhibited the maximum absorption wavelength at 515, 520, 580, 600, 540, 590 and 592 nm, respectively. The absorbance intensity of these aromatic amines decreased to 94, 95, 98, 90 and 88 nm with the increase of exposed time from 0 to 30 min, indicating the drastic decrease in the concentration of aromatic amines. A reasonably high degradation rate by 89-99% of aforementioned aromatic amines within 30 min are detected over the surface of CeO_2-TiO_2 NCs catalyst whereas, low photodegradation rates (1%, 3%, 6%, 8% and 10%) are obtained when aromatic amine photodegradation takes place over the surface commercial TiO_2 and CeO_2 catalysts under visible light illumination.

The maximum yield was observed as 99% for DCB aromatic amine while the yields for MOA and NA were calculated as 98% and 97%, respectively after 30 min

irradiation time at a power of 130 W UV (Figure 9). TDA was removed with a yield of 88% while the yield for TOA was recorded as 92% after 30 min photooxidation (Figure 9).

Aromatic amine metabolites

The formation of possible intermediates of 2,6-DMA, MOA, TDA, NA, TOA and DCB aromatic amines is illustrated in table 4. The intermediates of aromatic amines clearly reveal that the multiple fragmentation of aromatic amine macromolecule can lead the complete mineralization with the ending products of CO_2 and H_2O. DCB metabolites are N-acetyl-DCB and N,N'-diacetyl-DCB while N-phenylacetamide (acetanilide, NPA) and N-acetylated metabolites such as 5-OH-2-NA, 7-OH-2-

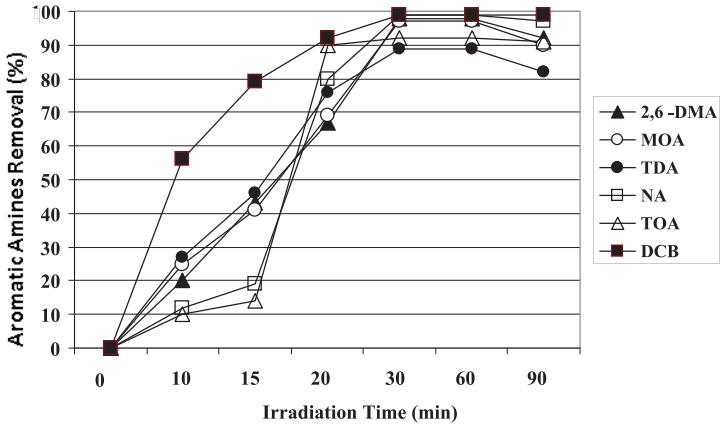

Figure 9 Photooxidation yields of decomposed TI ww for aromatic amines under 130W UV power, at 21°C with 15 mg/L CeO_2 - TiO_2 NCs, respectively.

Table 4: Removal efficiencies of aromatic amines metabolites after 10 min and 30 min irradiation with CeO_2-TiO_2 NCs under 130 W UV power.

Aromatic amines metabolites		After 10 min		After 30 min		
Names	Influent conc. (mg/L	Ce_2O_2-TiO_2 NCs conc. (mg/L)	Removal Eff. (%)	Ce_2O_2-TiO_2 NCs conc. (mg/L)	Removal Eff. (%)	Remaining conc. (mg/L)
DCB metabolites						
N-acetyl-DCB	200	92	54	8	96	8
N,N'-diacetyl-DCB	90	45	50	4.5	95	4.5
2, 6-DMA metabolites						
4-hydroxy-2,6-dimethyaniline	670	549.4	18	40.2	94	40.2
2-amino-3-methylbenzoic acid	450	369	18	13.5	97	13.5
2, 6-dimethylnitrosobenzene	100	81	19	7	93	7
3, 5-dimethyl-4-iminoquinone	34	27.2	20	1.7	95	1.7
MOA metabolites						
cis-1, 2-dihydroxy-3-methoxycyclohexa-3,5-diene	80	65.6	18	3.2	96	3.2
2-methoxyphenol	60	48.6	19	3	95	3
Catechol	20	16.2	19	1.4	93	1.4
Trace amounts of phenol	3	2.49	17	0.27	91	0.27
TDA metabolites						
4-acetylamino-2-aminotoluene	40	29.6	26	5.6	86	5.6
2,4-diacetylaminotoluene	80	60.8	24	12.8	84	12.8
4-acetylamino-2-aminobenzoic acid	40	31.2	22	7.6	81	7.6
2,4-diacetylaminobenzoic acid	10	7.8	22	1.7	83	1.7
TOA metabolites						
Benzidine	20	18.2	9	1.8	91	1.8
Mono-acethyl benzidine	120	110.4	8	12	90	12
Acethyl benzidine	30	27.6	8	3	90	3
$C1^{1-}$	25	23.25	7	3	88	3
Ethane	20	18.4	8	1.6	92	1.6
NA metabolites						
DMOB metabolites						

NA and 8-OH-2-NA were detected as NA metabolites. From 350 mg/L DCB 200 mg/L N-acetyl-DCB and 90 mg/L N,N'-diacetyl-DCB produced. 2000 mg/L 2,6-DMA metabolized principally to 670 mg/L 4-hydroxy-2,6-dimethylaniline (4-HDMA), to 450 mg/L 2-amino-3-methylbenzoic acid (2-AMBA), to 100 mg/L 2,6-dimethylnitrosobenzene and to 34 mg/L 3,5-dimethyl-4-imino-quinone during 130 W UV irradiation within 30 min photooxidation at 21˚C at 15 mg/L CeO_2-TiO_2 NCs at 15% CeO_2 mass ratio, respectively. 250 mg/L MOA was converted to 80 mg/L cis-l,2-dihydroxy-3-methoxycyclohexa-3,5-diene (anisole-2,3-dihydrodiol), to 60 mg/L 2-methoxyphenol, to 20 mg/L catechol, and to trace amounts of phenol (3 mg/L) after 30 min photodegradation at 21˚C with 15 mg/L CeO_2-TiO_2 NCs at 15% CeO_2 mass ratio, respectively. 360 mg/L TDA metabolites were 40 mg/L 4-acetylamino-2-aminotoluene, 80 mg/L 2,4-diacetylaminotoluene, their phenolic derivatives (40 mg/L 4-acetylamino-2-aminobenzoic acid and 10 mg/L 2,4-diacetylaminobenzoic acid) after 30 min irradiation times at 130 W UV power and at 21˚C, respectively. 300 mg/L TOA metabolites are 20 mg/L benzidine, 120 mg/L mono-acethyl benzidine, 30 mg/L acethyl benzidine, 25 mg/L Cl^{1-} and 20 mg/L ethane after 30 min photodegradation, at 21˚C with 15 mg/L CeO_2-TiO_2 NCs at 15% CeO_2 mass ratio, respectively.

DCB metabolites such as N-acetyl-DCB, N,N'-diacetyl-DCB removal efficiencies were 96% and 95%, after 30 min irradiation time (Table 4). 2,6-DMA metabolites such as 4-hydroxy-2,6-dimethylaniline, 2-amino-3-methylbenzoic acid, 2,6-dimethylnitrosobenzene, 3,5-dimethyl-4-imino quinone removal efficiencies were 94%, 97%, 93%, 95%, respectively after 30 min irradiation time (Table 4). MOA metabolites such as cis-1,2-dihydroxy-3-methoxycyclohexa-3,5-diene, 2-methoxyphenol, catechol, trace amount of phenol removal efficiencies were 96%, 95%, 93%, 91%, respectively, after 30 min irradiation time (Table 4). TDA metabolites such as 4-acetylamino-2-aminotoluene, 2,4-diacetylaminotoluene, 4-acetylamino-2-aminobenzoic acid, 2,4-diacetylaminobenzoic acid removal efficiencies were 86%, 84%, 81%, 83%, respectively, after 30 min irradiation time (Table 4). TOA metabolites such as benzidine, mono-acethyl benzidine, acethyl benzidine, Cl^{1-}, ethane removal efficiencies were 91%, 90%, 90%, 88%, 92%, respectively after 30 min irradiation time (Table 4). Reaction rates of aromatic amines metabolites (DCB, 2,6-DMA, NA, MOA and TOA) illustrated in figure 10.

Effect of increasing CeO_2-TiO_2 NCs concentrations with 5% and 15% CeO_2 mass ratios on the acute toxicity removal efficiencies in TI ww at increasing photodegradation time and temperature Effect of increasing CeO_2-TiO_2 NCs concentrations with 5% and 15% CeO_2 mass ratios on the microtox acute toxicity removal efficiencies in TI ww at increasing photodegradation time and temperature: The initial EC_{90} values at pH = 7.0 was found as 825 mg/L at 25˚C (Table 5, Set 1). After 60 min, 120 and 150 min of photodegradation the EC_{90} values decreased to EC_{55} = 414 mg/L to EC_{20} = 236 mg/L and to EC_{10} = 165 mg/L in CeO_2-TiO_2 NCs = 20 mg/L, at 5% CeO_2 mass ratio, at 30˚C (Table 5, Set 3). The toxicity removal efficiencies were 38.89%, 77.78% and 88.89% after 60 min, 120 and 150 min photodegradation times, respectively, in CeO_2-TiO_2 NCs = 20 mg/L, at 5% CeO_2 mass ratio, at 30˚C (Table 5, Set 3).

The EC_{90} values decreased to EC_{50}, to EC_{15} and to EC_5 after 60 min, 120 and 150 min photodegradation times, respectively, in TiO_2=20 mg/L, at 5% CeO_2 mass ratio, at 60˚C (Table 5, Set 3). The EC_{50}, the EC_{15} and the EC_5 values were measured as 550 mg/L, 540 and 500 mg/L, respectively, in CeO_2-TiO_2 NCs =20 mg/L, at 5% CeO_2 mass ratio, at 60˚C. The toxicity removal efficiencies were 44.44%, 83.33% and 94.44% after 60 min, 120 and 150 min photodegradation times, respectively, in CeO_2-TiO_2 NCs = 20 mg/L, at 5% CeO_2 mass ratio, at 60˚C (Table 5, Set 3). 94.44% maximum Microtox acute toxicity yield was found in CeO_2-TiO_2 NCs = 20 mg/L, at 5% CeO_2 mass ratio, after 150 min photodegradation time at 60˚C (Table 5, Set 3).

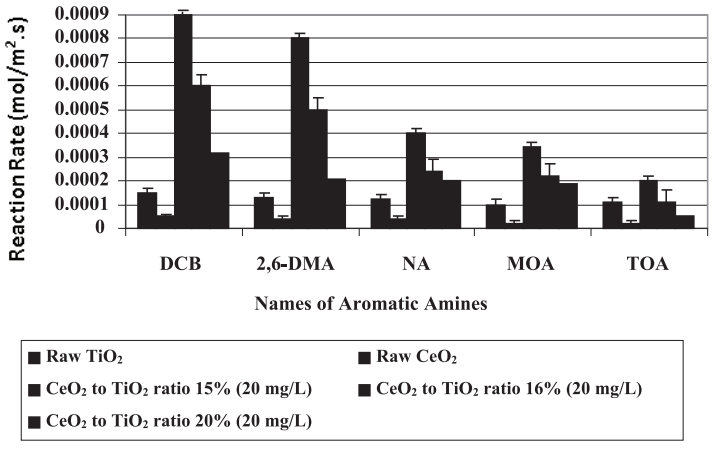

Figure 10 Reaction rates of aromatic amines metabolites (DCB, 2,6-DMA, NA, MOA and TOA).

Table 5: Effect of increasing CeO_2-TiO_2 NCs concentrations with 5% and 15% CeO_2 mass ratios on Microtox acute toxicity in TI ww at 130 W UV light irradiation, at 30˚C and at 60˚C, respectively.

No	Parameters	Microtox Acute Toxicity Values, *EC (mg/L)							
		25˚C							
		0. min		60. min		120. min		150. min	
		*EC_{90}		*EC		*EC		*EC	
1	Raw ww, control	825		EC_{70} = 510		EC_{60} = 650		EC_{50} = 640	
		30˚C				60˚C			
		0. min	60. min	120. min	150. min	0. min	60. min	120. min	150. min
		*EC_{90}	*EC	*EC	*EC	*EC_{90}	*EC	*EC	*EC
2	Raw ww, control	825	EC_{70} = 580	EC_{50} = 580	EC_{40} = 550	825	EC_{55} = 550	EC_{40} = 590	EC_{30} = 690
3	CeO_2-TiO_2 NCs = 15 mg/L at 5% CeO_2 mass ratio	825	EC_{60} = 422	EC_{25} = 241	EC_{15} = 168	825	EC_{55} = 419	EC_{20} = 266	EC_{10} = 150
	CeO_2-TiO_2 NCs = 15 mg/L at 15% CeO_2 mass ratio	825	EC_{60} = 421	EC_{25} = 239	EC_{15} = 167	825	EC_{55} = 414	EC_{20} = 232	EC_{10} = 161
	CeO_2-TiO_2 NCs = 20 mg/L at 5% CeO_2 mass ratio	825	EC_5 = 414	EC_{20} = 236	EC_{10} = 165	825	EC_{50} = 550	EC_{15} = 540	EC_5 = 500
	CeO_2-TiO_2 NCs = 20 mg/L at 15% CeO_2 mass ratio	825	EC_{65} = 408	EC_{30} = 230	EC_{20} = 162	825	EC_{60} = 403	EC_{25} = 218	EC_{15} = 148

*EC values were calculated based on COD_{dis} (mg/L).

The EC_{90} values decreased to EC_{60} = 422 mg/L to EC_{25} = 241 and to EC_{15} = 168 mg/L after 60 min, 120 and 150 min photodegradation times, respectively, in CeO_2-TiO_2 NCs = 15 mg/L, at 5% CeO_2 mass ratio, at 30˚C (Table 5, Set 3). The EC_{90} values decreased to EC_{60} = 421 mg/L to EC_{25} = 239 and to EC_{15}=167 mg/L after 60 min, 120 and 150 min photodegradation times, respectively, in CeO_2-TiO_2 NCs = 15 mg/L, at 15% CeO_2 mass ratio, at 30˚C. The EC_{90} values decreased to EC_{65} = 408 mg/L to EC_{30} = 230 and to EC_{20} = 162 mg/L after 60 min, 120 and 150 min photodegradation times, respectively, in CeO_2-TiO_2 NCs = 20 mg/L, at 15% CeO_2 mass ratio, at 30˚C. The Microtox acute toxicity removals were 83.33%, 83.33% and 77.78% in CeO_2-TiO_2 NCs = 15 mg/L at 5% CeO_2 mass ratio, in CeO_2-TiO_2 NCs = 15 mg/L at 15% CeO_2 mass ratio, and in CeO_2-TiO_2 NCs = 20 mg/L at 15% CeO_2 mass ratio, respectively, after 150 min photodegradation time at 30˚C. It was obtained an inhibition effect of CeO_2-TiO_2 NCs = 20 mg/L at 15% CeO_2 mass ratio to *Vibrio fischeri* after 150 min photodegradation time at 30˚C (Table 5, Set 3).

The EC_{90} values decreased to EC_{55} = 419 mg/L to EC_{20} = 266 and to EC_{10} = 150 mg/L after 60 min, 120 and 150 min photodegradation times, respectively, in CeO_2-TiO_2 NCs = 15 mg/L at 5% CeO_2 mass ratio, at 60˚C (Table 5, Set 3). The EC_{90} values decreased to EC_{55} = 414 mg/L to EC_{20} = 232 and to EC_{10} = 161 mg/L after 60 min, 120 and 150 min photodegradation times, respectively, in CeO_2-TiO_2 NCs = 15 mg/L, at 15% CeO_2 mass ratio, at 60˚C. The EC_{90} values decreased to EC_{60} = 403 mg/L to EC_{25} = 218 and to EC_{15} = 148 mg/L after 60 min, 120 and 150 min photodegradation times, respectively, in CeO_2-TiO_2 NCs = 20 mg/L, at 15% CeO_2 mass ratio, at 60˚C. The Microtox acute toxicity removals were 88.89%, 88.89% and 83.33% in CeO_2-TiO_2 NCs = 15 mg/L at 5% CeO_2 mass ratio, in CeO_2-TiO_2 NCs = 15 mg/L at 15% CeO_2 mass ratio and in CeO_2-TiO_2 NCs = 20 mg/L at 15% CeO_2 mass ratio, respectively, after 150 min photodegradation time at 60˚C. It was observed an inhibition effect of CeO_2-TiO_2 NCs = 20 mg/L at 15% CeO_2 mass ratio to *Vibrio fischeri* after 150 min photodegradation time at 60˚C (Table 5, Set 3).

Effect of increasing CeO_2-TiO_2 NCs concentrations with 5% and 15% CeO_2 mass ratios on the *Daphnia magna* acute toxicity removal efficiencies in TI ww at ıncreasing photodegradation time and temperature: The initial EC_{50} values were observed as 850 mg/L at 25˚C (Table 6, Set 1). After 60 min, 120 and 150 min of photodegradation the EC_{50} values decreased to EC_{30} = 350 mg/L to EC_{15} = 240 mg/L and to EC_{10} = 90 mg/L in CeO_2-TiO_2 NCs = 20 mg/L at 5% CeO_2 mass ratio, at 30˚C (Table 6, Set 3). The toxicity removal efficiencies were 40%, 70% and 80% after 60 min, 120 and 150 min photodegradation times, respectively, in in CeO_2-TiO_2 NCs = 20 mg/L at 5% CeO_2 mass ratio, at 30˚C (Table 6, Set 3).

The EC_{50} values decreased to EC_{25} to EC_{10} and to EC_5 after 60 min, 120 and 150 min photodegradation times, respectively, in CeO_2-TiO_2 NCs = 20 mg/L at 5% CeO_2 mass ratio, at 60˚C (Table 6, Set 3). The EC_{25}, the EC_{10} and the EC_5 values were measured as 150 mg/L, 60 and 375 mg/L, respectively, in CeO_2-TiO_2 NCs = 20 mg/L, at 5% CeO_2 mass ratio, at 60˚C. The toxicity removal efficiencies were 50%, 80% and 90% after 60 min, 120 and 150 min photodegradation times,

Table 6: Effect of increasing CeO_2-TiO_2 NCs concentrations with 5% and 15% CeO_2 mass ratios on *Daphnia magna* acute toxicity in TI ww, at 130 W UV light irradiation, at 30˚C and at 60˚C, respectively.

No	Parameters	*Daphnia magna* Acute Toxicity Values, *EC (mg/L)							
		25˚C							
		0. min		60. min		120. min		150. min	
		*EC_{50}		*EC		*EC		*EC	
1	Raw ww, control	850		EC_{45} = 625		EC_{40} = 370		EC_{30} = 155	
		30˚C				60˚C			
		0. min	60. min	120. min	150. min	0. min	60. min	120. min	150. min
		*EC_{50}	*EC	*EC	*EC	*EC_{50}	*EC	*EC	*EC
2	Raw ww, control	850	EC_{40} = 470	EC_{35} = 230	EC_{25} = 115	850	EC_{35} = 375	EC_{30} = 212	EC_{20} = 75
3	CeO_2-TiO_2 NCs = 15 mg/L at 5% CeO_2 mass ratio	850	EC_{35} = 450	EC_{20} = 145	EC_{15} = 260	850	EC_{30} = 130	EC_{15} = 425	EC_{10} = 340
	CeO_2-TiO_2 NCs = 15 mg/L at 15% CeO_2 mass ratio	850	EC_{35} = 450	EC_{20} = 175	EC_{15} = 100	850	EC_{30} = 425	EC_{15} = 140	EC_5 = 90
	CeO_2-TiO_2 NCs = 20 mg/L at 5% CeO_2 mass ratio	850	EC_{30} = 350	EC_{15} = 240	EC_{10} = 90	850	EC_{25} = 150	EC_{10} = 60	EC_5 = 375
	CeO_2-TiO_2 NCs = 20 mg/L at 15% CeO_2 mass ratio	850	EC_{40} = 300	EC_{25} = 170	EC_{20} = 52	850	EC_{35} = 250	EC_{20} = 110	EC_{15} = 11

*EC values were calculated based on COD_{dis} (mg/L).

respectively, in CeO_2-TiO_2 NCs = 20 mg/L, at 5% CeO_2 mass ratio, at 60˚C (Table 6, Set 3). 90% maximum *Daphnia magna* acute toxicity removal was obtained in CeO_2-TiO_2 NCs = 20 mg/L, at 5% CeO_2 mass ratio, after 150 min photodegradation time at 60˚C (Table 6, Set 3).

The EC_{50} values decreased to EC_{35} = 450 mg/L to EC_{20} = 145 and to EC_{15} = 260 mg/L after 60 min, 120 and 150 min photodegradation times, respectively, in CeO_2-TiO_2 = NCs = 15 mg/L, at 5% CeO_2 mass ratio, at 30˚C (Table 6, Set3). The EC_{50} values decreased to EC_{35} = 450 mg/L to EC_{20} = 175 and to EC_{15} = 100 mg/L after 60 min, 120 and 150 min photodegradation times, respectively, in CeO_2-TiO_2 NCs = 15 mg/L, at 15% CeO_2 mass ratio, at 30ºC. The EC_{50} values decreased to EC_{40} = 300 mg/L to EC_{25} = 170 and to EC_{20} = 52 mg/L after 60 min, 120 and 150 min photodegradation times, respectively, in CeO_2-TiO_2 NCs = 20 mg/L, at 15% CeO_2 mass ratio, at 30˚C. The *Daphnia magna* acute toxicity removals were 70%, 70% and 60% in CeO_2-TiO_2 NCs = 15 mg/L at 5% CeO_2 mass ratio, in CeO_2-TiO_2 = 15 mg/L at 15% CeO_2 mass ratio and in CeO_2-TiO_2 NCs = 20 mg/L at 15% CeO_2 mass ratio, respectively, after 150 min photodegradation time at 30˚C. It was observed an inhibition effect of CeO_2-TiO_2 = NCs = 20 mg/L at 15% CeO_2 mass ratio, to *Daphnia magna* after 150 min photodegration time at 30˚C (Table 6, Set 3).

The EC_{50} values decreased to EC_{30} = 130 mg/L to EC_{15} = 425 and to EC_{10} = 340 mg/L after 60 min, 120 and 150 min photodegradation times, respectively, in CeO_2-TiO_2 NCs = 15 mg/L, at 5% CeO_2 mass ratio, at 60˚C (Table 6, Set 3). The EC_{50} values decreased to EC_{30} = 425 mg/L to EC_{15} = 140 and to EC_5 = 90 mg/L after 60 min, 120 and 150 min photodegradation times, respectively, in CeO_2-TiO_2 NCs = 15 mg/L, at 15% CeO_2 mass ratio, at 60˚C. The EC_{50} values decreased to EC_{35} = 250 mg/L to EC_{20} = 110 and to EC_{15} = 11 mg/L after 60 min, 120 and 150 min photodegradation times, respectively, in CeO_2-TiO_2 NCs = 20 mg/L, at 15% CeO_2 mass ratio, at 60˚C. The *Daphnia magna* acute toxicity removals were 80%, 90% and 70% in CeO_2-TiO_2 NCs = 15 mg/L at 5% CeO_2 mass ratio, in CeO_2-TiO_2 NCs = 15 mg/L at 15% CeO_2 mass ratio and in CeO_2-TiO_2 NCs = 20 mg/L at 15% CeO_2 mass ratio, respectively, after 150 min photodegradation time at 60˚C. It was observed an inhibition effect of CeO_2-TiO_2 NCs = 20 mg/L at 15% CeO_2 mass ratio to *Daphnia magna* after 150 min photodegration time at 60˚C (Table 6, Set3).

Increasing the CeO_2-TiO_2 NCs concentrations from 15 mg/l to 20 mg/L did not have a positive effect on the decrease of EC_{50} values as shown in table 6 at Set 3. CeO_2-TiO_2 NCs concentrations > 20 mg/L decreased the acute toxicity removals by hindering the photodegradation process. Similarly, a significant contribution of increasing CeO_2-TiO_2 NCs concentration to acute toxicity removal at 60˚C after 150 min of photodegradation time was not observed. Low toxicity removals found at high CeO_2-TiO_2 NCs concentrations could be attributed to their detrimental effect on the *Daphnia magna* (Table 6, Set 3).

Direct Effects of CeO_2-TiO_2 NCs concentrations with 5% and 15% CeO_2 mass ratios on the acute toxicity of microtox and *Daphnia magna* in TI ww: The acute toxicity test was performed in the samples containing in CeO_2-TiO_2 NCs = 15 mg/L at 5% CeO_2 mass ratio, in CeO_2-TiO_2 NCs = 15 mg/L at 15% CeO_2 mass ratio, in CeO_2-TiO_2 NCs = 20 mg/L at 5% CeO_2 mass ratio and in CeO_2-TiO_2 NCs = 20 mg/L at 15% CeO_2 mass ratio, respectively. In order to detect the direct responses of Microtox and *Daphnia magna* to the increasing CeO_2-TiO_2 NCs concentrations with 5% ansd 15% CeO_2 mass ratios, the toxicity test were performed without TI ww. The initial EC values and the the EC_{50} values were measured in the samples

Table 7: The responses of Microtox and *Daphnia magna* acute toxicity tests in addition of increasing CeO_2-TiO_2 NCs concentrations with 5% and 15% CeO_2 mass ratios without TI ww after 150 min photodegradation time.

CeO_2-TiO_2 NCs Concentrations (mg/L)	Microtox Acute Toxicity Test			*Daphnia magna* Acute Toxicity Test		
	Initial EC_{50} values (mg/L)	Inhibitions after 150 min	EC values (mg/L)	Initial EC_{50} values (mg/L)	Inhibitions after 150 min	EC values (mg/L)
CeO_2-TiO_2 NCs = 15 mg/L at 5% CeO_2 mass ratio	EC_{10} = 25	-	-	EC_{10} = 40	-	-
CeO_2-TiO_2 NCs = 15 mg/L at 15% CeO_2 mass ratio	EC_{15} = 80	4	EC_1 = 4	EC_{20} = 100	6	EC_3 = 6
CeO_2-TiO_2 NCs = 20 mg/L at 5% CeO_2 mass ratio	EC_{20} = 150	6	EC_4 = 7	EC_{30} = 200	7	EC_6 = 12
CeO_2-TiO_2 NCs = 20 mg/L at 15% CeO_2 mass ratio	EC_{25} = 220	8	EC_6 = 10	EC_{40} = 300	10	EC_8 = 16

containing increasing CeO_2-TiO_2 NCs concentrations with 5% and 15% CeO_2 mass ratios, after 150 min photodegradation time. Table 7 showed the responses of Microtox and *Daphnia magna* to increasing TiO_2 concentrations.

The acute toxicity originating only from CeO_2-TiO_2 NCs = 15 mg/L at 5% mass ratio, to CeO_2-TiO_2 NCs = 15 mg/L at 15% mass ratio, to CeO_2-TiO_2 NCs = 20 mg/L at 5% mass ratio, to and to CeO_2-TiO_2 NCs = 20 mg/L at 15% mass ratio, respectively, were found to be low (Table 7). At CeO_2-TiO_2 NCs = 15 mg/L at 5% mass ratio did not exhibited toxicity to *Vibrio fischeri* and *Daphnia magna* before and after 150 min photodegration time. The toxicity atributed to the CeO_2-TiO_2 NCs = 15 mg/L at 15% mass ratio, to CeO_2-TiO_2 NCs = 20 mg/L at 5% mass ratio, to and to CeO_2-TiO_2 NCs = 20 mg/L at 15% mass ratio, respectively, were found to be low in the samples without TI ww for the test organisms mentioned above. The acute toxicity originated from the CeO_2-TiO_2 NCs decreased significantly to EC_1, EC_4 and EC_6 after 150 min photodegration time. Therefore, it can be concluded that the toxicity originating from the CeO_2-TiO_2 NCs is not significant and the real acute toxicity throughout photodegration was attributed to the TI ww, to their metabolites and to the photodegradation by-products (Table 7).

Conclusion

The results show that 15 mg/L CeO_2-TiO_2 nanocomposite with a CeO_2 mass ratio of 15%wt shows the highest photodegradation yield of color under both UV and visible-light irradiation, with maximum photo-degradation rates of 99% and 98.5%, respectively, after 30 min irradiation time. The maximum photooxidation yields for quercetin, fisetin and ellagic acid polyphenols were high (99%, 98% and 97%, respectively) while the yields for carminic acid, luteolin and curcumin polyphenols were sligthly low (88%, 82% and 80%, respectively). The maximum yield was observed as 99% for DCB aromatic amine while the yields for MOA and NA were calculated as 98% and 97%, respectively after 30 min irradiation time at a power of 130 W UV.

94.44% maximum Microtox acute toxicity yield was found in CeO_2-TiO_2 NCs = 20 mg/L, at 5% CeO_2 mass ratio, after 150 min photodegradation time at 60˚C. It was observed an inhibition effect of CeO_2-TiO_2 NCs = 20 mg/L at 15% CeO_2 mass ratio to *Vibrio fischeri* after 150 min photodegradation time at 30˚C and at 60˚C, respectively.

90% maximum *Daphnia magna* acute toxicity removal was obtained in CeO_2-TiO_2 NCs = 20 mg/L, at 5% CeO_2 mass ratio, after 150 min photodegradation time at 60˚C. It was obtained an inhibition effect of CeO_2-TiO_2 NCs = 20 mg/L at 15% CeO_2 mass ratio to *Daphnia magna* after 150 min photodegration time at 30˚C and 60˚C, respectively. As a result, it can be concluded that the toxicity originating from the CeO_2-TiO_2 NCs is not significant and the real acute toxicity throughout photodegration was attributed to the TI ww, to their metabolites and to the photodegradation by-products.

The CeO_2-TiO_2 NCs samples showed strong spectral response in the visible region and exhibited high photocatalytic activity under UV or visible irradiation compared with pure nano-TiO_2 and nano-CeO_2. It is an economical and environmentally sustainable method to utilize sunlight as a natural source of energy to treat dye wastewater through photocatalytic process.

Acknowledgment

This research study was undertaken in the Environmental Microbiology Laboratories at Dokuz Eylül University Engineering Faculty Environmental Engineering Department, İzmir, Turkey. The authors would like to thank this body for providing financial support.

References

1. Esplugas S, Yue PL, Pervez MI. Degradation of 4-chlorophenol by photolytic oxidation. Water Res. 1994;28:1323-1328.
2. Masten SJ, Davies SH. The use of ozonation to degrade organic contaminants in wastewaters. Environ Sci Technol. 1994 Apr 1;28(4):180A-5A. doi: 10.1021/es00053a718. PMID: 22657971.
3. Besson M, Descorme C, Bernardi M, Gallezot P, di Gregorio F, Grosjean N, Minh DP, Pintar A. Supported noble metal catalysts in the catalytic wet air oxidation of industrial wastewaters and sewage sludges. Environ Technol. 2010 Dec 1;31(13):1441-7. doi: 10.1080/09593331003628065. PMID: 21214003.
4. Chen X, Mao SS. Titanium dioxide nanomaterials: synthesis, properties, modifications, and applications. Chem Rev. 2007 Jul;107(7):2891-959. doi: 10.1021/cr0500535. Epub 2007 Jun 23. PMID: 17590053.
5. Jain R, Sikarwar S. Semiconductor-mediated photocatalyzed degradation of erythrosine dye from wastewater using TiO2 catalyst. Environ Technol. 2010 Nov;31(12):1403-10. doi: 10.1080/09593331003758789. PMID: 21121463.

6. Pouretedal HR, Beigy H, Keshavarz MH. Bleaching of Congo red in the presence of ZnS nanoparticles, with dopant of Co2+ ion, as photocatalyst under UV and sunlight irradiations. Environ Technol. 2010 Oct;31(11):1183-90. doi: 10.1080/09593330903414220. PMID: 21046948.
7. Vohra MS, Selimuzzaman SM, Al-Suwaiyan MS. NH4+-NH3 removal from simulated wastewater using UV-TiO2 photocatalysis: effect of co-pollutants and pH. Environ Technol. 2010 May;31(6):641-54. doi: 10.1080/09593331003596536. PMID: 20540426.
8. Linsebigler AL, Lu G, Yates JT. Photocatalysis on TiO_2 surfaces: Principles, mechanisms, and selected results. Chem Rev. 1995;95:735-758.
9. Asahi R, Morikawa T, Ohwaki T, Aoki K, Taga Y. Visible-light photocatalysis in nitrogen-doped titanium oxides. Science. 2001 Jul 13;293(5528):269-71. doi: 10.1126/science.1061051. PMID: 11452117.
10. Zheng Y, Shi E, Chen Z, Li W, Hu X. Influence of solution concentration on the hydrothermal preparation of titania crystallites. J Mater Chem. 2001;11:1547-1551.
11. Yamashita H, Harada H, Misaka J, Takeushi M, Ikeue K, Anpo M. Degradation of propanol diluted in water under visible light irradiation using metal ionimplanted titanium dioxide photocatalysts. Photoch Photobio A. 2002;148:257-261.
12. Yu JC, Zhang L, Zheng Z, Zhao J. Synthesis and characterization of phosphated mesoporous titanium dioxide with high photocatalytic activity. Chem Mater. 2003;15:2280-2286.
13. Wang W, Zhang J, Chen F, He D, Anpo M. Preparation and photocatalytic properties of Fe3+-doped Ag@TiO2 core-shell nanoparticles. J Colloid Interface Sci. 2008 Jul 1;323(1):182-6. doi: 10.1016/j.jcis.2008.03.043. Epub 2008 Apr 29. PMID: 18448112.
14. Chen F, Zou W, Qu W, Zhang J. Photocatalytic performance of a visible light TiO_2 photocatalyst prepared by a surface chemical modification process. Catal Commun. 2009;10:1510-1513.
15. Bhargava SK, Tardio J, Prasad J, Föger K, Akolekar DB, Grocatt SC. Wet oxidation and catalytic wet oxidation. Ind Eng Chem Res. 2006;45:1221-1258.
16. Massa P, Ivorra F, Haure P, Medina Cabello F, Fenoglio R. Catalytic wet air oxidation of phenol aqueous solutions by 1% Ru/CeO_2-Al_2O_3 catalysts prepared by different methods. Catal Commun. 2007;8:424-428.
17. Pavasupree S, Suzuki Y, Pivsa-Art S, Yoshikawa S. Preparation and characterization of mesoporous TiO_2-CeO_2 nanopowders respond to visible wavelength. J Solid State Chem. 2005;178:128-134.
18. Morimo T, Dutta G, Waghmare UV, Baidya T, Hegde MS, Priolkar KR, Sarode PR. Origin of enhanced reducibility/oxygen storage capacity of Ce1-xTixO_2 compared to CeO_2 or TiO_2. Chem Mater. 2006;18:3249-3256.
19. Li G, Zhang D, Yu JC. Thermally stable ordered mesoporous CeO2/TiO2 visible-light photocatalysts. Phys Chem Chem Phys. 2009 May 21;11(19):3775-82. doi: 10.1039/b819167k. Epub 2009 Feb 25. PMID: 19421491.
20. Li M, Zhang S, Lv L, Wang M, Zhang W, Pan B. A thermally stable mesoporous ZrO_2-CeO_2-TiO_2 visible light Photocatalyst. Chem Eng J. 2013;229:118-125.
21. Pirkarami A, Olya ME, Farshid SR. UV/Ni-TiO_2 nanocatalyst for electrochemical removal of dyes considering operating costs. Water Resour Ind. 2014;5:9-20.
22. Shao X, Lu W, Zhang R, Pan F. Enhanced photocatalytic activity of TiO_2-C hybrid aerogels for methylene blue degradation. Scientific Reports. 2018;3:1-9 doi: 10.1038/srep03018.
23. Subramonian W, Wu TY. Effect of enhancers and inhibitors on photocatalytic sunlight treatment of Methylene Blue, Water. Air. Soil. Poll. 225 (2014) 1922-1937.
24. Ji P, Tian B, Chen F, Zhang J. CeO2 mediated photocatalytic degradation studies of C.I. acid orange 7. Environ Technol. 2012 Feb-Mar;33(4-6):467-72. doi: 10.1080/09593330.2011.579183. PMID: 22629618.
25. Balavi H, Samadanian-Isfahani S, Mehrabani-Zeinabad M, Edrissi M. Preparation and optimization of CeO_2 nanoparticles and its application in photocatalytic degradation of Reactive Orange 16 dye. Powder Technol. 2013;249:549-555.
26. Zhao B, Shi B, Zhang X, Cao X, Zhang Y. Catalytic wet hydrogen peroxide oxidation of H-acid in aqueous solution with, TiO_2-CeO_2 and Fe/TiO_2-CeO_2 catalysts. Desalination. 2011;268:55-59.
27. Liu H, Wang M, Wang Y, Liang Y, Cao W, Su Y. Ionic liquid-templated synthesis of mesoporous CeO_2-TiO_2 nanoparticles and their enhanced photocatalytic activities under UV or visible light. J Photoch Photobio A. 2011;223:157-164.
28. Ameen S, Akhtar MS, Seo HK, Shin HS, Solution-processed CeO_2/TiO_2 nanocomposite as potent visible light photocatalyst for the degradation of bromophenol dye. Chem Eng J. 2014;247:193-198.
29. Baird RB, Eaton AD, Rice EW, editors. Standard Methods for the Examination of Water and Wastewater. 23rd ed. American Public Health Association (APHA), American Water Works Association (AWWA), Water Environment Federation (WEF). American Public Health Association 800 I Street, NW Washington DC: USA: 20001-3770. 2017.
30. Liu B, Zhao X, Zhang N, Zhao Q, He X, Feng J. Photocatalytic mechanism of TiO_2-CeO_2 films prepared by magnetron sputtering under UV and visible light. Surf Sci. 2005;595:203-211.
31. Riss A, Elser MJ, Bernardi J, Diwald O. Stability and photoelectronic properties of layered titanate nanostructures. J Am Chem Soc. 2009 May 6;131(17):6198-206. doi: 10.1021/ja810109g. PMID: 19358537.
32. Zubkov T, Stahl D, Thompson TL, Panayotov D, Diwald O, Yates JT Jr. Ultraviolet light-induced hydrophilicity effect on TiO2(110)(1 x 1). Dominant role of the photooxidation of adsorbed hydrocarbons causing wetting by water droplets. J Phys Chem B. 2005 Aug 18;109(32):15454-62. doi: 10.1021/jp058101c. PMID: 16852960.
33. Yang H, Zhang K, Shi R. Sol-gel synthesis and photocatalytic activity of CeO2/TiO2 nanocomposites. J Am Cer Soc. 2007;90:1370-1374.

How to cite this article: Öztekin R, Sponza DT. Photocatalytic Degradation of Polyphenols and Polyaromatic Amines in Textile Industry Wastewaters by Nano-Cerium Dioxide Doped Titanium Dioxide and the Evaluation of Acute Toxicity Assays with Microtox and *Daphnia magna*. J Biomed Res Environ Sci. 2022 Aug 09; 3(8): 852-866. doi: 10.37871/jbres1524, Article ID: JBRES1524, Available at: https://www.jelsciences.com/articles/jbres1524.pdf